Freiser, J. Am.

and T. L. Ricca,

Chapter 2

# New Excitation and Detection Techniques in Fourier Transform Ion Cyclotron Resonance Mass Spectrometry

**Alan G. Marshall [1,2], Tao-Chin Lin Wang[4], Ling Chen [1], and Tom L. Ricca [3]**

**[1]Department of Chemistry, Ohio State University, Columbus, OH 43210**
**[2]Department of Biochemistry, Ohio State University, Columbus, OH 43210**
**[3]Chemical Instrument Center, Ohio State University, Columbus, OH 43210**

FT/ICR experiments have conventionally been carried out with pulsed or frequency-sweep excitation. Because the cyclotron experiment connects mass to frequency, one can construct ("tailor") any desired frequency-domain excitation pattern by computing its inverse Fourier transform for use as a time-domain waveform. Even better results are obtained when phase-modulation and time-domain apodization are used. Applications include: dynamic range extension via multiple-ion ejection, high-resolution MS/MS, multiple-ion simultaneous monitoring, and flatter excitation power (for isotope-ratio measurements).

The analytically important features of Fourier transform ion cyclotron resonance (FT/ICR) mass spectrometry (1) have recently been reviewed (2-9): ultrahigh mass resolution (>1,000,000 at $m/z \leq 200$) with accurate mass measurement even in gas chromatography/mass spectrometry experiments; sensitive detection of low-volatility samples due to 1,000-fold lower source pressure than in other mass spectrometers; versatile ion sources (electron impact (EI), self-chemical ionization (self-CI), laser desorption (LD), secondary ionization (e.g., $Cs^+$-bombardment), fast atom bombardment (FAB), and plasma desorption (e.g., $^{252}Cf$ fission); trapped-ion capability for study of ion-molecule reaction connectivities, kinetics, equilibria, and energetics; and mass spectrometry/mass spectrometry (MS/MS) with a single mass analyzer and dual collision chamber.

## Ion Motion in Crossed Static Magnetic and Oscillating Electric Fields

The basic principle of FT/ICR mass spectrometry is that a moving ion in an applied static magnetic field undergoes circular motion, in a plane perpendicular to that field, at a "cyclotron" frequency, $\omega$,

[4]Current address: Section on Analytical Biochemistry, Building 10, Room 3D-40, National Institute of Mental Health, 9000 Rockville Pike, Bethesda, MD 20892

0097-6156/87/0359-0021$06.00/0

$$\vec{\omega}_c = q\vec{B}/m \qquad (1)$$

in which B is the magnetic field strength (Tesla), q is the ionic charge (Coul), and m is the ionic mass (kg). The cyclotron motion is excited and detected as shown schematically in Figure 1 (10). First, if an electric field oscillating (or rotating) at an angular frequency, $\omega (=2\pi\nu)$, in a plane perpendicular to the magnetic field axis, then "resonant" ions (i.e., those for which $\omega = \omega_c$) will be driven coherently forward in their orbits, so that their average ICR radius increases linearly with time. The resonant ions are said to be "excited" by the oscillating (typically radiofrequency) electric field. "Non-resonant" ions (i.e., for which $\omega \neq \omega_c$) will follow a complicated path whose long-term effect is to leave them essentially unmoved from their original positions.

Excited ion orbital radius is theoretically proportional to the product of the magnitude and duration of a resonant rf electric field (11). Moreover, the signal induced in an opposed pair of receiver plates of a trapped-ion cell is proportional to ICR radius (12). The time-domain signal magnitude (or frequency-domain spectral peak area) at a given cyclotron frequency is directly proportional to the number of ions of the corresponding m/z value. Thus, if there is no rf power at the ion's cyclotron resonance frequency (case A in Figure 1), then the incoherent cyclotron motion of a thermal ensemble of ions of common $\omega_c$ and translational energy but random phase (i.e., random angular position in their circular orbit) will induce zero signal in the receiver plates. Ions excited by a resonant rf electric field to an orbit that is large (e.g., 1 cm) but still within the cell boundaries (case B in Figure 1) will be detected with optimal sensitivity. Finally, ions resonantly excited to a radius larger than that of the ICR cell will be lost, or "ejected".

Thus, by appropriate scaling of the rf electric field magnitude at the ICR frequencies of ions of various m/z-ratios, we can suppress, excite and then detect, or eject ions at each m/z-ratio. The remaining problem is to design the optimal time-domain waveform to accomplish the desired combination of the effects shown at the bottom of Figure 1, over a wide mass range.

Figure 1. Fur
field directio
oscillating ra
opposed plates
frequency equa
electric field
whereas "off-r
thus other cyc
are left with
left). After
ICR orbital ra
electric field
undetected (A)
ejected (C).

## Excitation waveforms

First, it is important to appreciate that the detected ion cyclotron signal magnitude is (to a good approximation) directly proportional to the excitation magnitude, as we have previously demonstrated experimentally (13,14). Thus, in contrast to sector or quadrupole mass spectrometers, it is not necessary to compute the detailed trajectories of the ions in order to determine the effect of those trajectories upon the detector. In other words, we need only characterize the excitation magnitude spectrum (i.e., how much power reaches ions at each ICR frequency) in order to know how much signal to expect at the receiver (for a given number of ions at that cyclotron frequency).

The frequency-domain spectra of four kinds of time-domain excitation waveforms are shown in Figure 2. A simple rectangular radiofrequency pulse was the waveform used to produce the very first FT/ICR signals (1), and is still useful for single-frequency ejection of ions having a narrow range of m/z-values. However, the width of its corresponding frequency-domain "sinc" function (Fig.2, top right)

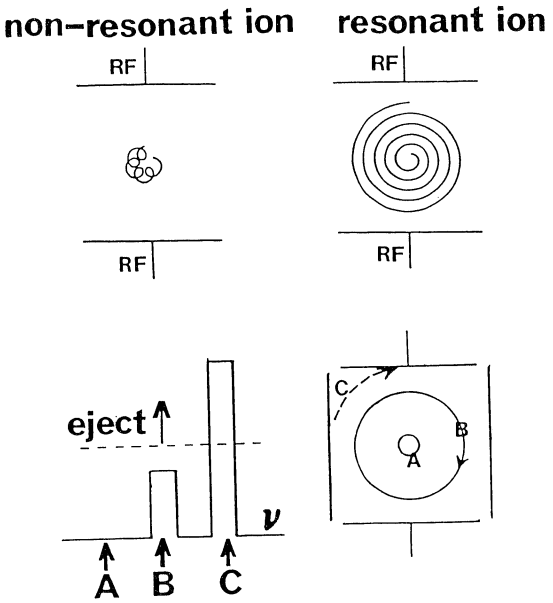


Figure 1. Fundamentals of ICR excitation. The applied magnetic field direction is perpendicular to the page, and a sinusoidally oscillating radiofrequency electric field is applied to two opposed plates (see upper diagrams). Ions with cyclotron frequency equal to ("resonant" with) that of the applied rf electric field will be excited spirally outward (top right), whereas "off-resonant" ions of other mass-to-charge ratio (and thus other cyclotron frequencies) are excited non-coherently and are left with almost no net displacement after many cycles (top left). After the excitation period (lower diagrams), the final ICR orbital radius is proportional to the amplitude of the rf electric field during the excitation period, to leave ions undetected (A), excited to a detectable orbital radius (B), or ejected (C).

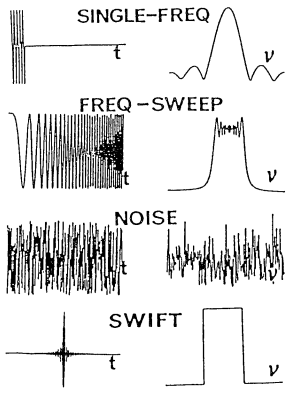


Figure 2. Time-domain excitation waveforms (left) and corresponding frequency-domain magnitude-mode spectra (right) of four excitation waveforms used in FT/ICR. A time-domain rectangular rf pulse gives a "sinc" excitation spectrum in the frequency-domain. A time-domain frequency-sweep gives a complex profile described by Fresnel integrals. Single-scan time-domain noise gives noise in the frequency-domain. Finally, Stored Waveform Inverse Fourier Transform (SWIFT) excitation can provide an optimally flat excitation spectrum (see Figure 3 for details).

varies inversely with the duration of the rf pulse. As a result, pulsed rf excitation is unsuitable for the broadband excitation needed to span a typical mass spectral range (say, $18 < m/z < 600$): an rf pulse of very short duration (<0.1 μs), and thus an impractically high magnitude (>10,000 V/cm) would be needed (11).

Therefore, the second (15) and virtually all subsequent FT/ICR experiments have been performed via frequency-sweep excitation, in which the time-domain rf waveform is swept linearly across the frequency bandwidth corresponding the the $m/z$-range of interest. Although successful in exciting ICR signals over a wide mass range at relatively low excitation magnitude (ca. 10 V(p-p)/cm), the problems with frequency-swept excitation are evident in Figure 2. First, the excitation magnitude varies significantly (up to ca. ±25% for typical bandwidth and sweep rate) over the mass range of interest. Thus, equally abundant ions of different $m/z$-ratio can exhibit different apparent intensities (11), and isotope-ratio measurements cannot easily be quantitated.

One could propose pseudorandom (16) or random (17) noise as an excitation source. However, a single time-domain noise waveform produces unacceptably large magnitude variation in the frequency-domain (see Figure 2). The frequency-domain envelope for random noise can be smoothed by frequency-domain averaging of sufficiently large number of scans, but the time required (ca. 10 hr) would be unacceptably long. Flat power can also be extracted from decoding the results of a series of linearly independent pseudorandom sequences (e.g., Hadamard sequences (18)), but again a large number of scans is required.

The best approach, adapted from an earlier proposal by Tomlinson and Hill (19), is to specify the desired frequency-domain excitation profile in advance, and then syntheize its corresponding time-domain representation directly via inverse Fourier transformation. The result of the Tomlinson and Hill procedure is shown at the bottom of Figure 2, in which a perfectly flat, perfectly selective frequency-domain excitation is produced by the time-domain waveform obtained via inverse Fourier transformation of the desired spectrum.

## Stored Waveform Inverse Fourier Transform (SWIFT) Excitation

Unfortunately, the result shown in Figure 2 corresponds to time-shared (i.e., essentially simultaneous) excitation/detection, so that the (discrete) frequencies sampled by the detector are the same as those initially specified in synthesis of the time-domain transmitter signal. However, FT/ICR is more easily conducted with temporally separated excitation and detection periods. In practical terms, the result is that for FT/ICR, we need to know the excitation magnitude spectrum at all frequencies, not just those (equally-spaced) discrete frequencies that defined the desired excitation spectrum.

The left-hand column of Figure 3 illustrates the basic SWIFT procedure. A constant-phase (see below) excitation spectrum is first defined at N equally-spaced discrete frequencies. Inverse Fourier transformation then generates the corresponding digitized time-domain waveform, which may be translated, point by point at a constant rate, by a digital-to-analog converter, amplified, and applied to the transmitter plates of an ICR trapped-ion cell. The time-domain signal is then padded with N zeroes (18,20) before Fourier transformation to give the magnitude-mode spectrum shown at the

s (left) and corre-
pectra (right) of
A time-domain
tion spectrum in the
-sweep gives a complex
ingle-scan time-domain
Finally, Stored
excitation can provide
Figure 3 for details).

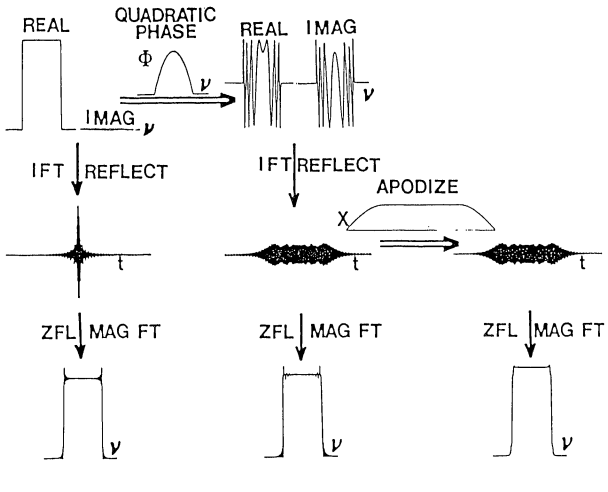


Figure 3. Digital synthesis of a Stored Waveform Inverse Fourier Transform (SWIFT) excitation. Although direct inverse discrete Fourier transform of a constant-phase frequency-domain spectrum (top left) gives a time-domain waveform (middle left) with good frequency-domain uniformity and selectivity (bottom left), the dynamic range of that time-domain waveform can be inconveniently large. Therefore, the original excitation spectrum is first phase-encoded (in this case, quadratically) to give the in-phase and 90°-out-of-phase spectra specified by their magnitude and phase at each discrete frequency (top middle). Inverse Fourier transformation then gives a time-domain waveform (center) with reduced dynamic range and the same final excitation magnitude spectrum (bottom middle). Finally, time-domain apodization (middle right) further smoothes the final excitation magnitude spectrum (bottom right). The time-domain waveforms (middle row) were zero-filled before Fourier transformation, to define the frequency-domain spectral values both at and between the initially specified discrete frequencies of the spectra in the top row of the Figure.

bottom left of Figure 3. Zero-filling effectively interpolates the final frequency-domain spectrum to reveal its values at frequencies equally spaced between the initially specified frequencies. The non-rectangular shape of the final spectrum is simply a consequence of the classical uncertainty principle: namely, that one cannot measure (or specify) a frequency more accurately than about $\pm(1/T)$ Hz via a time-domain waveform of duration, T.

Time-domain waveforms generated from a constant-phase initial spectrum by the SWIFT procedure just described have been successfully applied to broad-band excitation, windowed excitation, and multiple-ion monitoring (11), and to multiple-ion ejection for enhancement of FT/ICR dynamic range (21) as described below. However, three practical problems are associated with the relatively large time-domain vertical dynamic range (see middle left in Figure 3) that can result from that procedure. First, the time-domain dynamic range may exceed the linear response range of the analog transmitter circuitry. Second, the time-domain dynamic range may exceed the digital dynamic range of the digital-to-analog converter (e.g., 12-bit) or even the host computer (e.g., 20 bit) in which the time-domain waveform must be stored. Third, because most of the transmitter power is concentrated into such a short burst, an rf amplifier with much more power (factor of up to 400 compared to frequency-sweep excitation) may be needed.

## Phase Modulation

As discussed in detail in ref. 22, the origin of the large time-domain dynamic range produced by constant-phase SWIFT lies in the common phase relationship between all of the specified frequency-domain spectral components, much as for the centerburst in an FT/IR interferogram or the large initial signal in an NMR free-induction decay (23). The time-domain dynamic range may therefore be reduced by somehow scrambling the relative phases of the initially specified frequency components, as shown in the top row of Figure 3. Phrased another way, what is needed is to distribute the excitation spectrum between its "real" (i.e., in-phase) and "imaginary" (90°-out-of-phase) components, rather than putting all of the signal into the "real" spectrum.

A simple phase-scrambling scheme is a quadratic variation of phase with frequency (see Figure 3, middle column), in which one must be careful not to violate the Nyquist criterion: i.e., the rate of change of phase with frequency, $d\phi/d\nu$, may not vary by more than $\sim$180° from one discrete frequency to the next in the initial spectrum. Subject to that constraint, a larger phase variation, $d\phi/d\nu$, will produce a smaller time-domain dynamic range. The wider the frequency bandwidth for a given time-domain excitation period, the greater will be the potential reduction in time-domain dyanmic range resulting from phase-encoding.

## Apodization

Although phase-encoding solves the problems associated with large time-domain dyanmic range in SWIFT excitation, the final frequency-domain spectrum still exhibits noticeable oscillation in magnitude at frequencies near the limits of the bandwidth. The final spectrum can be smoothed significantly by prior weighting ("apodization") of the

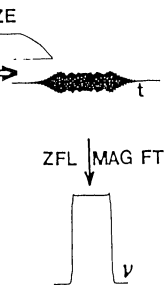


aveform Inverse Fourier
rect inverse discrete
uency-domain spectrum
iddle left) with good
y (bottom left), the
can be inconveniently
spectrum is first
) to give the in-phase
their magnitude and
le). Inverse Fourier
veform (center) with
xcitation magnitude
omain apodization
excitation magnitude
waveforms (middle row)
ation, to define the
nd between the
f the spectra in the

stored time-domain waveform before it is sent to the transmitter. Any of several weighting functions designed to bring the time-domain signal smoothly to zero at both ends of its period is suitable. The result for one such apodization function is shown in the right-hand column of Figure 3. The final frequency-domain excitation magnitude spectrum is considerably smoother than without apodization.

General applications

Figure 4 shows ideal and actual excitation magnitude-mode spectra for representative mass spectral applications. For example, quantitation of relative numbers of ions of different m/z-ratios requires ideally flat excitation power over the mass range of interest. The leftmost segments of the spectra of Figure 4 show that stored-waveform excitation offers much flatter power for such applications (e.g., isotope-ratio measurements, gas-phase ion-molecule equilibrium constants, etc.).

Truly simultaneous multiple-ion monitoring (rightmost segments of the spectra in Figure 4) can be performed via ICR. Unlike single-channel (e.g., sector or quadrupole) mass spectrometers, in which ions of only a narrow range of m/z-values can be detected at a given instant, FT/ICR offers inherently broadband detection, so that all ions in a given mass range may be detected simultaneously. Thus, by exciting only the frequencies corresponding to the m/z-values of interest, FT/ICR automatically provides simultaneous multiple-ion monitoring. In the (typical) situation shown in Figure 4, SWIFT is much more selective than a series of frequency-sweeps because the SWIFT time-domain power is left on for the entire time-domain excitation period, whereas the frequency-sweep power must be turned on and off once for each mass range to be monitored.

Dynamic range extension

As discussed in detail in ref. 21, a major problem in FT/ICR is the limited mass spectral dynamic range (factor of ~1000:1). Briefly, it is not easy to detect fewer than ~100 ions at easily managed chamber pressures ($\geq 10^{-9}$ torr); alternatively, the spectrum can be distorted by Coulomb forces when more than ~100,000 ions are present.

Consequences of the dynamic range limit are well-illustrated in Figure 5. The normal broad-band FT/ICR mass spectrum of perfluoro-tri-n-butylamine exhibits several strong peaks. Simple expansion of the vertical scale renders some of the small peaks visible, but their presence and quantitation is made difficult by the Coulomb broadening and overlap from abundant ions of nearby m/z-ratios.

An obvious solution is to eject selectively all of the most abundant ions, leaving only the small peaks of interest. As argued from Figure 4, multiple frequency-sweeps are not sufficiently selective for this purpose. However, SWIFT tailored ejection of the most abundant ions (23 in this case) removes the broadening and overlap from the large peaks. The resultant spectrum of the less abundant ions (bottom of Figure 5) exhibits better mass resolution (because Coulomb broadening has been reduced) and flatter baseline

Figure 4. Co
spectrum (top
verse plates)
transverse pl
(bottom) wave
before Fourie
excitation ma
and selectivi

Figure 5. Dy
ejection. To
spectrum of p
in which the
at m/z = 503
same sample,
of the (23) p
threshold of
original spec
noise, and f
spectrum.

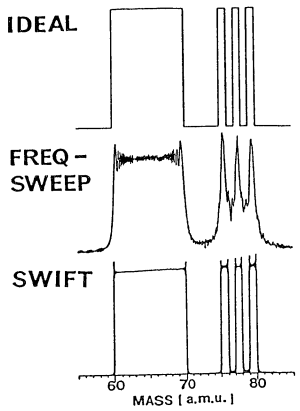


Figure 4. Comparison of a theoretical magnitude-mode excitation spectrum (top) with those detected (on one pair of cell transverse plates) during transmission (on the other pair of cell transverse plates) of a frequency-sweep (middle) or SWIFT (bottom) waveform. The time-domain signals were zero-filled once before Fourier transformation to reveal the full shape of the excitation magnitude spectrum. Note the much improved uniformity and selectivity for SWIFT compared to frequency-sweep excitation.

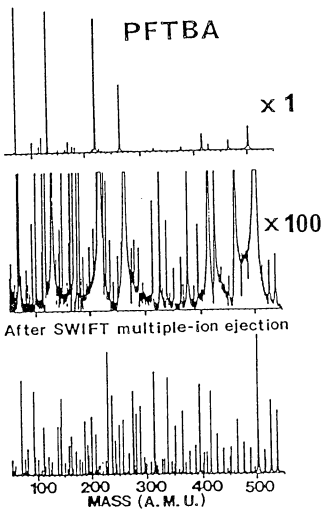


Figure 5. Dynamic range enhancement via SWIFT multiple-ion ejection. Top: Normal broad-band heterodyne-mode FT/ICR mass spectrum of perfluorotri-n-butylamine. Middle: Same spectrum, in which the vertical scale has been expanded such that the peak at $m/z$ = 503 is full scale. Bottom: FT/ICR mass spectrum of the same sample, obtained following prior SWIFT multiple-ion ejection of the (23) peaks whose magnitude-mode peak heights exceeded a threshold of 1.6 % of the height of the biggest peak in the original spectrum. Note the higher mass resolution, reduced noise, and flatter baseline in the SWIFT multiple-ion ejected spectrum.

(because the large peaks (and their broad shoulders) have been eliminated). Moreover, because most of the originally formed ions are removed, it is possible to increase the receiver gain and/or increase the number of initially formed ions to increase dynamic range further.

High-resolution MS/MS

The potentially ultrahigh mass resolution of FT/ICR detection was one of its earliest appreciated advantages (24). Moreover, the potential of FT/ICR for MS/MS with a single mass spectrometer has been exploited extensively (see especially refs. 5 and 8, citing examples up to MS/MS/MS/MS/MS). In MS/MS via FT/ICR, a typical event sequence might be the selective ejection of all but one ion (i.e., the first "MS"), followed by collision-induced (collision-activated) dissociation in the presence of a steady or pulsed collision gas, followed by broad-band excitation and detection of the mass spectrum of daughter ions (i.e., the second "MS). Although mass resolution in the second "MS" is detector-limited (and therefore potentially ultrahigh), mass resolution in the first "MS" has been limited by the poor selectivity of frequency-sweep excitation (e.g., Figure 4).

The introduction of the SWIFT technique (10,14,21,22) makes possible FT/ICR frequency-domain excitation with the same mass resolution as has already been demonstrated for FT/ICR detection, provided only that sufficient computer memory is available to store a sufficiently long time-domain waveform. When ejection must be performed with ultrahigh mass resolution over a wide mass range, a simple solution is to use two successive SWIFT waveforms: first, a broad-band low-resolution excitation designed to eject ions except over (say) a 1 amu mass range; and then a second SWIFT waveform, heterodyned to put $\geq$ 8K data points spanning a mass range of 1-2 amu.

Finally, SWIFT excitation also offers a way to compress the sequence even further by combining the ejection and excitation stages. As shown in Figure 6 for two isotopic ions of nominal mass 92, from electron ionization of toluene at 0.5 x $10^{-9}$ torr, it is possible to eject the more abundant ion while exciting its narrowly resolved neighbor. Each excitation spectrum was defined by quadratically modulated real (8K) imaginary (8K) frequency-domain points, to give a 16K time-domain stored data set, transmitted over a period of 65.920 ms to give a 125 kHz bandwidth centered at a radiofrequency carrier frequency of 500 kHz (10).

Figure 6. S
very similar
tion of tolu
experimental
the magnitud
signal. Top
tailored SWI
Bottom: FT/
excitation/
excited whil
1:5 in excit
-m$_1$) >20,000
high-resolut

Conclusion

Stored Waveform Inverse Fourier Transform (SWIFT) excitation for FT/ICR is a newly implemented technique which includes all other excitation waveforms as subsets. Compared to prior excitation waveforms (e.g., frequency-sweep), SWIFT offers flatter power with greater mass resolution and the possibility of magnitude steps (without additional delays or switching transients) in the excitation spectrum. Briefly, SWIFT increases the mass resolution for FT/ICR excitation to the ultrahigh mass resolution already demonstrated for FT/ICR detection.

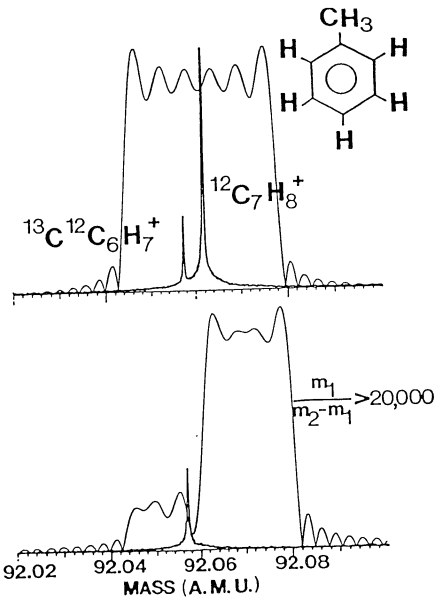


Figure 6. Simultaneous FT/ICR excitation/ejection of two ions of very similar mass-to-charge ratio, produced via electron ionization of toluene. In each plot, the heavy line represents the experimental FT/ICR mass spectrum, and the light line represents the magnitude-mode excitation spectrum used to produce that ICR signal. Top: $^{12}C_6H_8^+$ and $^{13}C^{12}C_6H_7^+$ are excited with uniformly tailored SWIFT excitation extending from m/z = 92.04 to 92.08. Bottom: FT/ICR mass spectrum obtained via SWIFT simultaneous excitation/ ejection, in which $^{13}C^{12}C_6H_7^+$ at mass 92.058 is excited while $^{12}C_6H_8^+$ at mass 92.062 is ejected, at a ratio of 1:5 in excitation magnitude. The ultrahigh selectivity ($(m_2/(m_2-m_1)$ >20,000) of such experiments should be valuable for high-resolution MS/MS (see text).

GLOSSARY

m/z: ionic mass-to-charge ratio, in which m is in atomic mass units and z is in multiples of the electronic charge.

Signal amplitude: maximum vertical displacement from equilibrium for a sinusoidally oscillating waveform. Signal amplitude is thus half of the peak-to-peak vertical displacement.

Signal power: square of signal amplitude. For a transverse (e.g., electromagnetic) wave, the power is the energy deposited per unit time per unit cross-sectional area.

Signal magnitude: square root of signal power.

Sinc function: sinc(x) = sin(x)/x. The sinc function is most often encountered as the (frequency-domain) Fourier transform of a (time-domain) rectangular pulse.

Windowed excitation: selective excitation with uniform power over specified frequency range(s), and with zero power over other frequency range(s) (window(s)) for ICR signal suppression.

For other specialized terms of Fourier transform spectroscopy (e.g., interferogram, centerburst, etc.), see ref. 23.

Acknowledgments

This work was supported by grants (to A.G.M.) from the U.S.A. Public Health Service (N.I.H. 1 ROl GM-31683) and The Ohio State University.

Literature Cited

1. Comisarow, M. B.; Marshall, A. G. Chem. Phys. Lett. 1974, 25, 282-283.
2. Marshall, A. G. Acc. Chem. Res. 1985, 18, 316-322.
3. Gross, M. L.; Rempel, D. L. Science (Washington, D.C.) 1984, 226, 261-268.
4. Wanczek, K. P. Int. J. Mass Spectrom. Ion Proc. 1984, 60, 11-60.
5. Freiser, B. S. Talanta 1985, 32, 697-708.
6. Laude, D. A., Jr.; Johlman, C. L.; Brown, R. S.; Weil, D. A.; Wilkins, C. L. Mass Spectrom. Rev. 1986, 5, 107-166.
7. Russell D. H. Mass Spectrom. Rev. 1986, 5, 167-189.
8. Nibbering, N. M. M. Comments At. Mol. Phys. 1986, 18, 223-234.
9. Comisarow, M. B. Anal. Chim. Acta 1985, 178, 1-15.
10. Chen, L.; Marshall, A. G. submitted for publication.
11. Comisarow, M. B. J. Chem. Phys. 1978, 69, 4097-4104.
12. Marshall, A. G.; Roe, D. C. J. Chem. Phys. 1980, 73, 1581-1590.
13. Marshall, A. G.; Wang, T.-C. L.; Ricca, T. L. Chem. Phys. Lett. 1984, 105, 233-236.
14. Marshall, A. G.; Wang, T.-C. L.; Ricca, T. L. J. Amer. Chem. Soc. 1985, 107, 7893-7897.
15. Comisarow, M. B.; Marshall, A. G. Chem. Phys. Lett. 1974, 26, 489-490.



16. Ijames, 58-62.
17. Marshal 1984, 1
18. Marshal in Chem pp. 1-4
19. Tomlinso 1775-178
20. Comisaro
21. Wang, T. 58, 293
22. Chen, L. Anal. Ch
23. Marshall Kuwana,
24. Comisaro 119.

RECEIVED June

16. Ijames, C. F.; Wilkins, C. L. Chem. Phys. Lett. 1984, 108, 58-62.
17. Marshall, A. G.; Wang, T.-C. L.; Ricca, T. L. Chem. Phys. Lett. 1984, 108, 63-66.
18. Marshall, A. G., In "Fourier, Hadamard, and Hilbert Transforms in Chemistry"; Marshall, A. G., Ed.; Plenum: New York, 1982; pp. 1-43.
19. Tomlinson, B. L.; Hill, H. D. W. J. Chem. Phys. 1973, 59, 1775-1784.
20. Comisarow, M. B.; Melka, J. D. Anal. Chem. 1979, 51, 2198-2203.
21. Wang, T.-C. L.; Ricca, T. L.; Marshall, A. G. Anal. Chem. 1986, 58, 2935-2938.
22. Chen, L.; Wang, T.-C. L.; Ricca, T. L.; Marshall, A. G., Anal. Chem. 1987, 59, 449-454.
23. Marshall, A. G. In Physical Methods in Modern Chemical Analysis; Kuwana, T., Ed.; Academic: New York, 1983; pp. 57-135.
24. Comisarow, M. B.; Marshall, A. G. J. Chem. Phys. 1976, 64, 110-119.

RECEIVED June 15, 1987